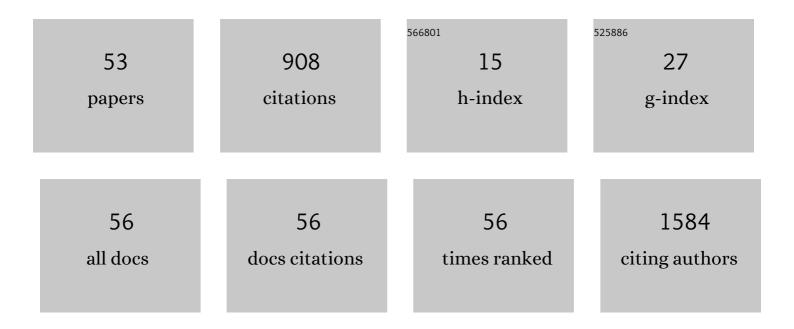
Lisa C Adams

List of Publications by Year in descending order

Source: https://exaly.com/author-pdf/400323/publications.pdf Version: 2024-02-01



LISA C ADAMS

#	Article	IF	CITATIONS
1	Deep learning for accurately recognizing common causes of shoulder pain on radiographs. Skeletal Radiology, 2022, 51, 355-362.	1.2	16
2	Evaluation of potential tissue heating during percutaneous drill-assisted bone sampling in an in vivo porcine study. Skeletal Radiology, 2022, 51, 829-836.	1.2	2
3	ADAMTS4-specific MR probe to assess aortic aneurysms in vivo using synthetic peptide libraries. Nature Communications, 2022, 13, .	5.8	6
4	Prostate158 - An expert-annotated 3T MRI dataset and algorithm for prostate cancer detection. Computers in Biology and Medicine, 2022, 148, 105817.	3.9	17
5	Highly accurate classification of chest radiographic reports using a deep learning natural language model pre-trained on 3.8 million text reports. Bioinformatics, 2021, 36, 5255-5261.	1.8	41
6	Targeting the Extracellular Matrix in Abdominal Aortic Aneurysms Using Molecular Imaging Insights. International Journal of Molecular Sciences, 2021, 22, 2685.	1.8	10
7	Deep-Learning-Based Diagnosis of Bedside Chest X-ray in Intensive Care and Emergency Medicine. Investigative Radiology, 2021, 56, 525-534.	3.5	14
8	Effect of Doxycycline on Survival in Abdominal Aortic Aneurysms in a Mouse Model. Contrast Media and Molecular Imaging, 2021, 2021, 1-9.	0.4	3
9	De Novo Radiomics Approach Using Image Augmentation and Features From T1 Mapping to Predict Gleason Scores in Prostate Cancer. Investigative Radiology, 2021, 56, 661-668.	3.5	18
10	Deep learning for detection of radiographic sacroiliitis: achieving expert-level performance. Arthritis Research and Therapy, 2021, 23, 106.	1.6	37
11	Correlation of Native Liver Parenchyma T1 and T2 Relaxation Times and Liver Synthetic Function Tests: A Pilot Study. Diagnostics, 2021, 11, 1125.	1.3	2
12	Improving CT accuracy in the diagnosis of COVID-19 in a hospital setting. Clinical Imaging, 2021, 76, 1-5.	0.8	4
13	Molecular MR Imaging of Prostate Cancer. Biomedicines, 2021, 9, 1.	1.4	29
14	Microscopic multifrequency magnetic resonance elastography of ex vivo abdominal aortic aneurysms for extracellular matrix imaging in a mouse model. Acta Biomaterialia, 2021, 140, 389-389.	4.1	2
15	Quantitative 3D Assessment of ⁶⁸ Ga-DOTATOC PET/MRI with Diffusion-Weighted Imaging to Assess Imaging Markers for Gastroenteropancreatic Neuroendocrine Tumors: Preliminary Results. Journal of Nuclear Medicine, 2020, 61, 1021-1027.	2.8	12
16	Native T1 Mapping Magnetic Resonance Imaging as a Quantitative Biomarker for Characterization of the Extracellular Matrix in a Rabbit Hepatic Cancer Model. Biomedicines, 2020, 8, 412.	1.4	7
17	The role of visceral adiposity in the severity of COVID-19: Highlights from a unicenter cross-sectional pilot study in Germany. Metabolism: Clinical and Experimental, 2020, 110, 154317.	1.5	146
18	Native T1 mapping for assessment of the perilesional zone in metastases and benign lesions of the liver. Scientific Reports, 2020, 10, 12889.	1.6	1

LISA C ADAMS

#	Article	IF	CITATIONS
19	Comparing different deep learning architectures for classification of chest radiographs. Scientific Reports, 2020, 10, 13590.	1.6	109
20	Intracellular accumulation capacity of gadoxetate: initial results for a novel biomarker of liver function. Scientific Reports, 2020, 10, 18104.	1.6	0
21	Simultaneous molecular MRI of extracellular matrix collagen and inflammatory activity to predict abdominal aortic aneurysm rupture. Scientific Reports, 2020, 10, 15206.	1.6	14
22	Value of susceptibility-weighted imaging for the assessment of angle measurements reflecting hip morphology. Scientific Reports, 2020, 10, 20899.	1.6	5
23	Molecular MR-Imaging for Noninvasive Quantification of the Anti-Inflammatory Effect of Targeting Interleukin-1β in a Mouse Model of Aortic Aneurysm. Molecular Imaging, 2020, 19, 153601212096187.	0.7	2
24	Multiparametric Assessment of Changes in Renal Tissue after Kidney Transplantation with Quantitative MR Relaxometry and Diffusion-Tensor Imaging at 3 T. Journal of Clinical Medicine, 2020, 9, 1551.	1.0	19
25	Subregion Radiomics Analysis to Display Necrosis After Hepatic Microwave Ablation—A Proof of Concept Study. Investigative Radiology, 2020, Publish Ahead of Print, 422-429.	3.5	5
26	Noninvasive imaging of vascular permeability to predict the risk of rupture in abdominal aortic aneurysms using an albumin-binding probe. Scientific Reports, 2020, 10, 3231.	1.6	14
27	Is lung density associated with severity of COVID-19?. Polish Journal of Radiology, 2020, 85, 600-606.	0.5	6
28	MR Angiography of the Head/Neck Vascular System in Mice on a Clinical MRI System. Contrast Media and Molecular Imaging, 2019, 2019, 1-9.	0.4	1
29	Dual-probe molecular MRI for the in vivo characterization of atherosclerosis in a mouse model: Simultaneous assessment of plaque inflammation and extracellular-matrix remodeling. Scientific Reports, 2019, 9, 13827.	1.6	13
30	Perioperative and oncologic outcome in patients treated for renal cell carcinoma with an extended inferior vena cava tumour thrombus level II-IV. Aktuelle Urologie, 2019, , .	0.3	2
31	Use of quantitative T2 mapping for the assessment of renal cell carcinomas: first results. Cancer Imaging, 2019, 19, 35.	1.2	25
32	Concurrent Molecular Magnetic Resonance Imaging of Inflammatory Activity and Extracellular Matrix Degradation for the Prediction of Aneurysm Rupture. Circulation: Cardiovascular Imaging, 2019, 12, e008707.	1.3	32
33	Assessment of the extracellular volume fraction for the grading of clear cell renal cell carcinoma: first results and histopathological findings. European Radiology, 2019, 29, 5832-5843.	2.3	15
34	Improved visualisation of hepatic metastases in gadoxetate disodium-enhanced MRI: Potential of contrast-optimised (phase-sensitive) inversion recovery imaging. PLoS ONE, 2019, 14, e0213408.	1.1	6
35	Native T1 Mapping as an In Vivo Biomarker for the Identification of Higher-Grade Renal Cell Carcinoma. Investigative Radiology, 2019, 54, 118-128.	3.5	31
36	Evaluation of osseous cervical foraminal stenosis in spinal radiculopathy using susceptibility-weighted magnetic resonance imaging. European Radiology, 2019, 29, 1855-1862.	2.3	17

LISA C ADAMS

#	ARTICLE	IF	CITATIONS
37	Differentiation of Predominantly Osteoblastic and Osteolytic Spine Metastases by Using Susceptibility-weighted MRI. Radiology, 2019, 290, 146-154.	3.6	19
38	Quantitative susceptibility mapping across two clinical field strengths: Contrastâ€ŧoâ€noise ratio enhancement at 1.5T. Journal of Magnetic Resonance Imaging, 2018, 48, 1410-1420.	1.9	11
39	Sclerotic bone lesions as a potential imaging biomarker for the diagnosis of tuberous sclerosis complex. Scientific Reports, 2018, 8, 953.	1.6	13
40	Evaluation of vertebral body fractures using susceptibility-weighted magnetic resonance imaging. European Radiology, 2018, 28, 2228-2235.	2.3	13
41	Renal cell carcinoma with venous extension: prediction of inferior vena cava wall invasion by MRI. Cancer Imaging, 2018, 18, 17.	1.2	56
42	Magnetic resonance imaging in heart failure, including coronary imaging: numbers, facts, and challenges. ESC Heart Failure, 2018, 5, 3-8.	1.4	4
43	Contrast-Enhanced Magnetic Resonance Angiography Using a Novel Elastin-Specific Molecular Probe in an Experimental Animal Model. Contrast Media and Molecular Imaging, 2018, 2018, 1-9.	0.4	2
44	Non-alcoholic fatty liver disease in underweight patients with inflammatory bowel disease: A case-control study. PLoS ONE, 2018, 13, e0206450.	1.1	21
45	Feasibility of gadoxetate disodium enhanced 3D T1 MR cholangiography (MRC) with a specific inversion recovery prepulse for the assessment of the hepatobiliary system. PLoS ONE, 2018, 13, e0203476.	1.1	1
46	Assessing venous thrombus in renal cell carcinoma: preliminary results for unenhanced 3D-SSFP MRI. Clinical Radiology, 2018, 73, 757.e9-757.e19.	0.5	4
47	Assessment of intracranial meningiomaâ€associated calcifications using susceptibilityâ€weighted MRI. Journal of Magnetic Resonance Imaging, 2017, 46, 1177-1186.	1.9	16
48	Evaluation of sclerosis in Modic changes of the spine using susceptibility-weighted magnetic resonance imaging. European Journal of Radiology, 2017, 88, 148-154.	1.2	12
49	Detection of vessel wall calcifications in vertebral arteries using susceptibility weighted imaging. Neuroradiology, 2017, 59, 861-872.	1.1	5
50	Diagnostic performance of susceptibility-weighted magnetic resonance imaging for the detection of calcifications: A systematic review and meta-analysis. Scientific Reports, 2017, 7, 15506.	1.6	23
51	In Vivo High-Frequency Ultrasound for the Characterization of Thrombi Associated with Aortic Aneurysms in an Experimental Mouse Model. Ultrasound in Medicine and Biology, 2017, 43, 2882-2890.	0.7	3
52	Diagnostic accuracy of susceptibility-weighted magnetic resonance imaging for the evaluation of pineal gland calcification. PLoS ONE, 2017, 12, e0172764.	1.1	10
53	Treatment effect of mTOR-inhibition on tissue composition of renal angiomyolipomas in tuberous sclerosis complex (TSC). PLoS ONE, 2017, 12, e0189132.	1.1	12